Using temperature as observable of the frequency response of RF CMOS amplifiers

E. Aldrete-Vidrio[1], M.A. Salhi[2], J. Altet[1*], S. Grauby[2] ,D. Mateo[1], H. Michel[2], L. Clerjaud[2], J.M. Rampnoux[2], A. Rubio[1], W. Claeys[2], S. Dilhaire[2].

[1]*Electronic Engineering Department, Universitat Politècnica de Catalunya, Barcelona, Spain*
[2]*CPMOH, Université de Bordeaux I, Bordeaux, France*
[*]*pepaltet@eel.upc.edu*

Abstract

The power dissipated by the devices of an integrated circuit can be considered a signature of the circuit's performance. Without disturbing the circuit operation, this power consumption can be monitored by temperature measurements on the silicon surface. In this paper, the frequency response of a RF LNA is observed by measuring spectral components of the sensed temperature. Results prove that temperature can be used to debug and observe figures of merit of analog blocks in a RF IC. Experimental measurements have been done in a 0.25μm CMOS process. Laser probing techniques have been used as temperature sensors; specifically, a thermoreflectometer and a Michaelson interferometer.

Key Words- Thermal test, analog test, RF test, system debug, temperature measurements.

1. Introduction

Nowadays, analog CMOS testing techniques are facing many challenges due to scaling and design evolution. Due to the huge amount of devices and the considerable number of blocks that constitute a radio frequency system-on-chip integrated circuit (RFIC-SoC), its characterization and test is usually done at system level, measuring high level figures of merit such as Bit Error Rate (BER) or Error Vector Magnitude (EVM) [1]. If during the first phases of development, some samples of an RFIC-SoC are found not to meet the required system specifications, then they go to the debugging phase, where an explanation of this misbehavior is searched for. A deviation of any of the expected figures of merit of the basic blocks that integrate the system (low noise amplifier (LNA), mixer, filters, etc….) has probably occurred. Being able of measuring individually each analog block of the system can help in finding their electrical figures of merit such as, frequency response, central frequency, gain, non-linearity, etc. This allows the right modification of the faulty block during the next design phase in order to meet the system level specifications.

The LNA is often the most critical block in the RF front-end since its figures of merit may affect the performance of the entire transceiver. Different alternative solutions have been proposed to increase the observability of internal nodes of this individual block in the RFIC. Some techniques have focused on built-in self test (BIST) reusing components of the front-end, such as analog-to-digital converter (ADC) based test [3], VCO-based test [7] and oscillator-based scheme [2]. Other techniques include built-in testers (BIT) together with the circuit under test (CUT), for instance a test amplifier (TA) was used in [4] to perform loop-back test; a band-gap reference, and RF peak detectors are used [5]. RMS detectors [6], test attenuators, multiplexers and switches [18], I_{DD} built-in current sensors and V_{bias} sensors [19], and built-in power sensors [20] have been some of the strategies used. Main requirements for these on-chip monitoring circuitry are low area overhead, minimum increase in the pinout, and an almost inappreciable loading effect on the CUT. Although the various BIST and BIT proposed schemes, they would still degrade the performance of de CUT because they are embedded or attached in the critical RF signal paths [4-6], [18-20]. Moreover, the requirements of the built-in testers are comparable to those for the CUT [2-3], [7].

In digital circuits, the use of the silicon surface temperature as a test observable, usually for failure analysis, is a solution that provides information about the state of the CUT [8]. For instance, hot spots are usually related to the presence of defects in CMOS digital circuits [8]. The interest of measuring temperature is twofold. First, the CUT is not electrically loaded: the temperature measuring sensor receives the information thanks to the silicon substrate thermal coupling, and then the performance of the CUT is unaffected. Second, measuring the silicon surface temperature has been largely reported in the literature, e.g., [9-10], and many mature sensing strategies are available. Thanks to these properties the use of temperature to test and characterize analog circuits is of a great interest. In [11-12] the relation between the figures of merit of an analog block and its power dissipation is analyzed. As an example, [11] shows the existent relation between the frequency response of an amplifier and its power dissipation as well as the conditions that have to be met to observe this frequency response by temperature measurements.

In this paper we present experimental measurements of the technique proposed in [11]. The CUT is a 0.25 μm CMOS RF-LNA. Temperature has been measured by using laser probing techniques. Nevertheless, the technique can

1530-1877/08 $25.00 © 2008 IEEE
DOI 10.1109/ETS.2008.15

be used with other temperature sensing strategies, such as the use of embedded temperature sensors. The results show that the frequency response of the amplifier and its central frequency can be observed by measuring the temperature at a given point close to the amplifier.

The paper is organized as follows. Section II reviews the principle of the proposed technique. Section III describes the designed IC prototype. A brief review of the laser probing techniques is presented in section IV. Section V describes the measurement setup. Section VI shows the experimental results. Finally, section VII concludes the paper.

2. Monitoring the frequency response of amplifiers by measuring temperature

Fig. 1 depicts an IC structure with a CUT and the area where the temperature is measured. The temperature can be measured either by using built-in or off-chip sensors. When the CUT is biased, a temperature waveform is measured at the temperature sensing area due to the thermal coupling through the silicon substrate. Fig. 1 also shows a model for this thermal coupling, which relates the power dissipated $P(t)$ by the devices of the CUT and the temperature $T(t)$. This coupling can be modeled with a transfer function $H_c(f)$, that behaves as a low pass filter with a cut-off frequency in the order of tens to hundreds of kilohertz [17]. The exact value of the cut-off frequency depends on the distance between the CUT and the temperature sensing area and on the geometry and nature of the heating source (size, thermal diffusivity,…).

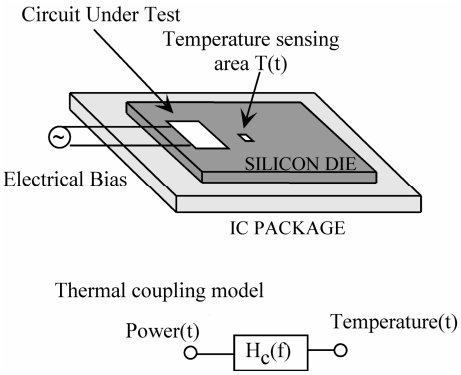

Figure 1: Thermal coupling between the Circuit Under Test and the temperature sensing area.

Let us suppose that the CUT is a linear circuit electrically biased with a sinusoidal function of frequency f, and that it does not need DC bias, e.g., a resistor. Fig. 2 shows the spectrums of the electrical bias, the power dissipated by the CUT ($P=V^2/R$), and the sensed temperature. As we can see, temperature is a means to observe the power dissipated by the CUT, but filtered by the transfer function $H_c(f)$. In this example, as the cut-off frequency of the thermal coupling is lower than the frequency $2f$, only the temperature component at DC can be sensed [12].

Fig. 3 shows the three spectrums when the CUT is driven by an electrical bias composed by two tones of frequencies f_1 and f_2. The frequencies f_1 and f_2 can be in the range of MHz to GHz, but if (f_2-f_1) is small enough. i.e., in the band of the thermal coupling effect in the IC, the spectral component of the power dissipated at (f_2-f_1) is observable by measuring the spectral component of the temperature at the same frequency (f_2-f_1). It is important to emphasize that the magnitude and phase of the spectral component of the power dissipated at (f_2-f_1) depends on the value of amplitude and phase of the electrical signals (voltage and current) present in the CUT at f_1 and f_2. Consequently, we can say that the phase and amplitude of the spectral component of the sensed temperature at the frequency (f_2-f_1) is an observable of the electrical signals present at the CUT at the high frequencies f_1 and f_2.

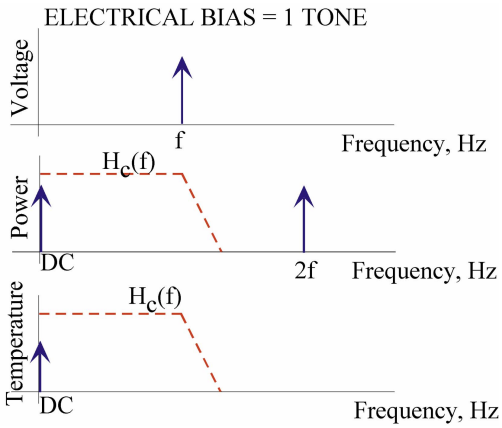

Figure 2: Spectrum of the electrical bias applied to the CUT (one tone), power waveform dissipated by the CUT and sensed temperature. Thermal transfer function $H_c(f)$ is also shown.

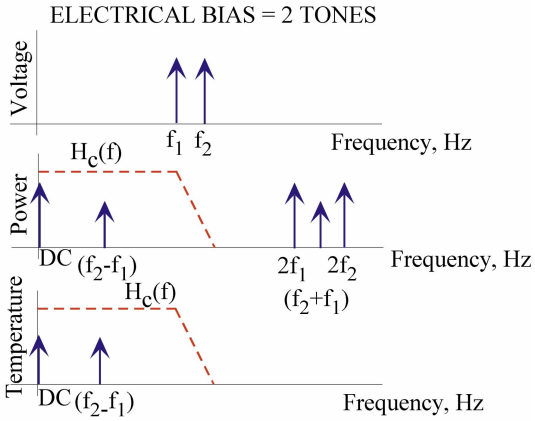

Figure 3: Spectrum of the electrical bias applied to the CUT (two tones), power waveform dissipated by the CUT and sensed temperature. The thermal transfer function $H_c(f)$ is also shown.

The value of (f_2-f_1) has to meet several criteria: first, it has to be in the working band of the temperature sensor used. In addition, it can provide a natural partitioning of the

IC, as the attenuation of the thermal coupling in the silicon substrate increases as the frequency of the spectral component measured increases and as the distance between the dissipating device and the temperature observation area is larger.

The case of the CUT being a linear amplifier is analyzed in [11-12]. In those papers it is proven that the amplitude of the power dissipated at (f_2-f_1) depends on the gain of the amplifier at frequencies f_1 and f_2. If both frequencies are close enough, these two gains have almost the same value and the amplitude of the power dissipated at (f_2-f_1) is proportional to the gain to either f_1 or f_2.

Therefore, if two tones of frequencies f_1 and f_2 are applied to a linear amplifier and the values of f_1 and f_2 are swept in the whole working band of the amplifier but keeping the value of (f_2-f_1) constant, e.g., 1 kHz, the evolution of the amplitude of the spectral component of the sensed temperature at 1 kHz is an observable of the frequency response of the amplifier, since its amplitude is proportional to the gain of the amplifier at frequencies f_1 and f_2.

The effect of the amplifier's non-linearities in the temperature measurements is also analyzed in [11-12].

3. Description of the designed IC

Fig. 4 shows a circuit-level description of a typical Low Noise Amplifier [13]. It is a single-ended cascode LNA with inductive source degeneration.

The LNA has been fabricated in TSMC's 0.25 µm MS/RF deep n-well CMOS technology through MOSIS, which provides single poly layer and five metals layers for inter-connections. The photograph of the chip is shown in Fig. 5. The layout area (core) is 1.25 x 1.25 mm^2. The size of transistors MNC and MNA are 200µm/0.25µm, formed by interdigitated structures (20 fingers) with an area of 224 µm^2 each. Since the attenuation of the thermal coupling increases as the distance between the dissipating device and the temperature sensing area increases, transistors MNC and MNA are separated about 350 µm. The purpose of this layout is to be able to observe the power dissipated by each transistor by temperature measurements avoiding thermal interfaces between them.

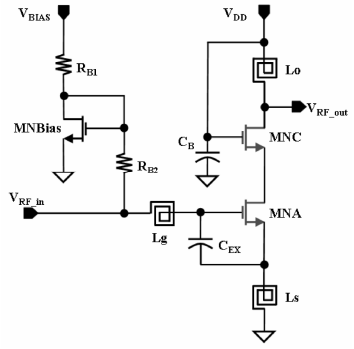

Figure 4: Inductively source degenerated LNA.

4. Laser probing techniques

Two different laser probing techniques have been used as temperature sensors: laser reflectometer and a Michaelson interferometer. Its principles and application examples are widely published in the literature, e.g., [10]. In this section, we present the basic principles of these techniques to introduce them to a non-expert reader.

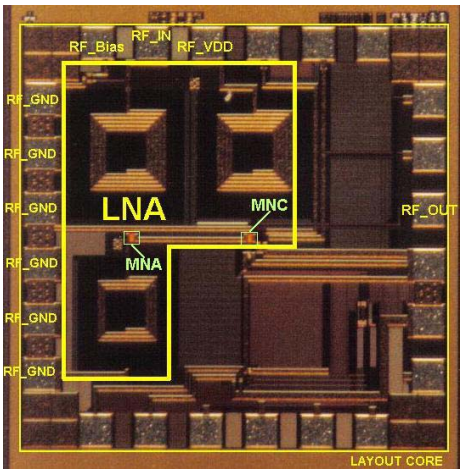

Figure 5: Chip die photograph.

Thermoreflectance [14] exploits the proportionality between the relative variation of reflectivity ΔR/R at the surface of a device and its temperature change ΔT. The proportionality coefficient is called thermoreflectance coefficient, κ in relation (1). If a laser beam is focused on the silicon surface and the reflected light is sensed with a photodiode, measuring the relative variations of the photocurrent, $\Delta I/I$, we deduce the relative variation of reflectivity which can be linearly related to variations of the temperature, ΔT, of the area to which the laser points:

$$\frac{\Delta I}{I} = \frac{\Delta R}{R} = \kappa \times \Delta T \qquad (1)$$

The constant κ depends on the material and the light wavelength. Typical values of κ can be found in the relevant literature. However, when the laser beam reaches the silicon surface through silicon dioxide and passivation layers, this coefficient is affected by a scaling factor that can be greater or smaller than unity, depending on the thickness of these layers [15]. Usually a calibration stage is needed to obtain the exact value of κ. Results reported in [16] show the laser probe to be a fast surface thermometer (dc to 150 MHz) with an excellent lateral resolution (1 µm) and large dynamics (ΔT can be measured from 10^2 to 10^{-3} K).

In an interferometer, a laser beam is split into a reference arm and a probe arm, ended with a mirror and the sample under measure, respectively. The two reflected beams interfere in a photodiode. The phase of the reflected

beams depends on the length of each optical path. Whereas the beam coming from the mirror has a constant optical path (and therefore, a constant phase), the phase of the light coming from the sample can be written as $\varphi=\varphi_0+\Delta\varphi$. The term $\Delta\varphi$ is related to surface displacements, which in our case are induced by thermal expansion associated with temperature changes. The current I given by the photodiode can be written as:

$$I = \frac{\phi}{2}(1 + M \cdot \cos\Delta\varphi)$$
$$\Delta\varphi = \frac{2\pi}{\lambda}\Delta z \qquad (2)$$

where Φ is the light intensity, λ is the laser wavelength, M is a constant that depends on the reflectivity of the sample under study and the phase shift $\Delta\varphi$ is related to the thermal expansion Δz of the sample. As the setup is similar to the reflectometer one, the same bandwidth and lateral resolution are obtained. A sensitivity in the order of fm is reported in [16]. As a summary, the measurement of both ΔR and $\Delta\varphi$ are proportional to the value of temperature increase ΔT of the area pointed by the laser.

5. Measurement setup

Chip-on-Board technology was use for experimentation purpose. The bare silicon die is glued directly to the printed circuit board substrate and then connected by bonding aluminum wires. This reduces the impact of the packages in the RF figures of merit of the amplifier and allows having direct visual access to the silicon die in order to perform the temperature measurements with the laser probes.

A. Electrical

Fig. 6 shows the experimental setup for electrical measurements. The vector signal generator (VSG) and the spectrum analyzer have been used to obtain the 1 dB compression point and the gain of the amplifier as a function of the frequency.

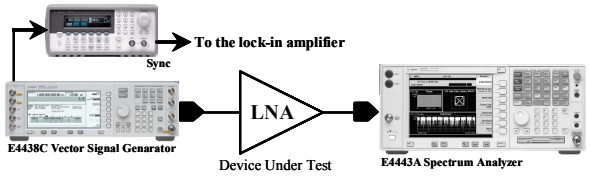

Figure 6: Electrical measurement setup.

The VSG can as well generate two tones of frequencies f_1 and f_2, and it allows sweeping the frequency of both tones keeping the value of (f_2-f_1) constant. The low frequency generator is synchronized with the high frequency generator and provides the external reference to a lock-in amplifier, i.e., a periodic signal at frequency (f_2-f_1). The synchronization of the high frequency and the low frequency generators allow to lock and to stabilize the frequency of the three signals generated. This stability is fundamental for the success of the measurements.

B. Optical

1) Interferometer: the laser probe is a homodyne stabilized Michaelson interferometer. The laser is a single frequency CW laser (λ=532nm). It is split by a Polarizing Beam Spliter (PBS) into a reference arm and a probe arm ended respectively by a pizomirror and the sample under test. The area lighted by the laser when focused on the sample has a radius of less than 5 µm. The piezomirror can be moved by a piezoactuator controlled by the feedback loop of the active stabilization. This active stabilization seeks, on the one hand, to bias the interferometer in its maximum sensitivity operating point, and on the other hand, to compensate low frequency displacements of the optical setup due to temporal drifts that otherwise may be interpreted as thermal dilatations. The two reflected beams interfere on a photodiode, see Fig. 7. The lock-in amplifier receives as input the signal delivered by the detector and measures the amplitude and phase of the spectral component of this input signal at the frequency provided by the low frequency generator, which is at (f_2-f_1). Therefore, the readings provided by the lock-in amplifier are related to the amplitude and phase of the desired spectral component of the temperature at the silicon surface area pointed by the laser.

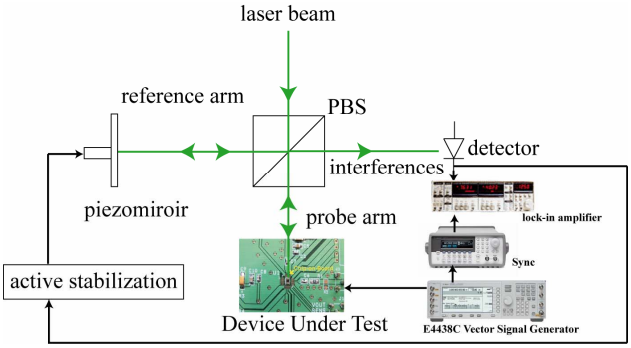

Figure 7: Optical measurement setup.

2) Reflectometer: the experimental setup is the same as the described for the interferometer, but now there is no reference arm. No interferences occur and the photodiode directly measures the amplitude changes of the reflected laser beam generated by variations of the reflectivity of the area pointed by the laser. As in the previous case, the signal delivered by the detector is the input to the lock-in amplifier, which gives us a reading related to the amplitude and phase of the spectral component of the temperature at (f_2-f_1) of the area pointed by the laser.

6. Experimental Results

Figure 8 shows measurements when only one sinusoidal signal is applied to the amplifier's input. The figure shows the amplifier's gain as a function of the frequency of the input signal. Three different measurements are superimposed, for three different amplitudes of the input signal: - 10 dBm, 0 dBm and 5 dBm. As it can be seen, the gain is very similar for input powers -10 dBm and 0 dBm.

As the 1dB compression point (@870 MHz) is 1 dB, when the input power is 5 dBm the amplifier is beyond its linear range and its gain decreases. As it can be seen, the amplifier presents gain in the band of 500 MHz to 1.5 GHz, with a central frequency around 900 MHz.

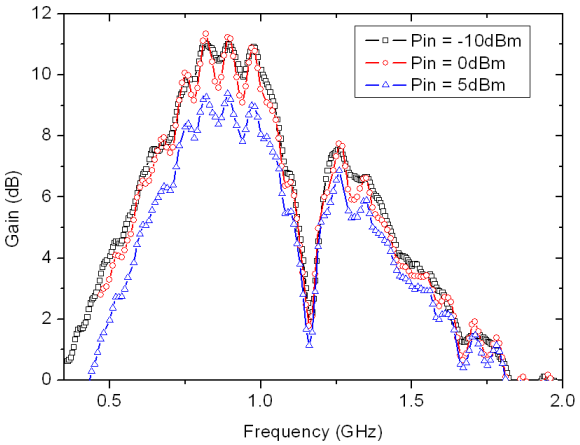

Figure 8: Gain of the LNA.

Fig. 9 compares electrical and thermal measurements when two tones of frequencies f_1 and f_2 are applied at the input of the LNA. To obtain this graphic the value of f_1 and f_2 has been swept from 500 MHz to 1.6 GHz, but keeping the value of (f_2-f_1) equal to 1012 Hz during the whole sweeping. We have obtained this plot in automated way, at a rate of 1 sample every 50 s. The x-axis shows the value of $(f_1+f_2)/2$. The right y-axis shows the gain of the amplifier calculated using the input and output tones at f_1. The left y-axis shows the amplitude of the spectral component of the signal provided by the photodiode at the frequency of 1012 Hz for different values of f_1 and f_2. This measurement is proportional to the amplitude of the same spectral component of the temperature waveform at the area pointed by the laser. This plot has been obtained by reflectomety when the laser beam has been focused on the silicon surface at 25 µm from the center of transistor MNC, see Fig. 5. Due to the spacing between the transistors MNA and MNC in the layout, and the chosen value of (f_2-f_1) (thermal coupling attenuate with the frequency and the distance), we can ensure that this measure is only due to the power dissipated by the transistor MNC.

If we compare both plots, similar shape is observed in the frequency band of 500 MHz to 1.1 GHz. From temperature measurements a central frequency of 830 MHz can be estimated. The notch in the electrical measurement is at around 1.16 GHz, whereas in the thermal measurements it is at around 1.10 GHz. We have observed that for frequency values higher than 1.5 GHz, the thermal measurements trend to 0.

Figures 10 and 11 compare temperature measurements performed at (f_2-f_1) with the frequency response of the amplifier in the frequency band of 500 MHz to 1.10 MHz. In these cases the amplitude of the input tones is -5 dBm. Fig. 10 shows measurements obtained with the reflectometer when (f_2-f_1) is 1012 Hz, whereas Fig. 11 shows measurements obtained with the interferometer when (f_2-f_1) is 5012 Hz (due to the active stabilization, the interferometer has higher sensitivity for working frequencies higher than 3 KHz).

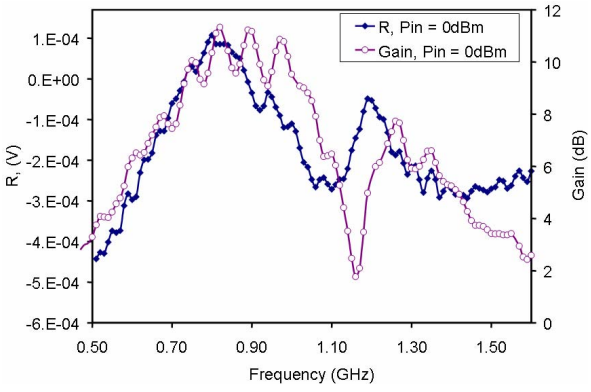

Figure 9: Gain (right y-axis) and amplitude of the reflectometric measurements (left y-axis) at (f_2-f_1) = 1012 Hz as a function of $(f_1+f_2)/2$.

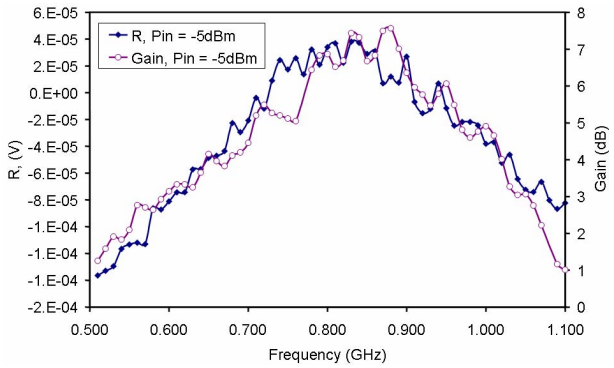

Figure 10: Gain (right y-axis) and amplitude of the reflectometric measurements (left y-axis) at (f_2-f_1) = 1012 Hz as a function of $(f_1+f_2)/2$

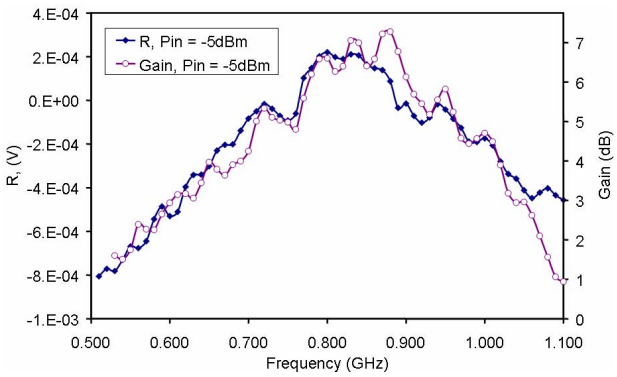

Figure 11: Gain (right y-axis) and amplitude of the interferometric measurements (left y-axis) at (f_2-f_1) = 5012 Hz as a function of $(f_1+f_2)/2$

As it can be seen, the signal obtained from temperature measurements has good agreement with the frequency

response of the amplifier in this frequency band. It is noticeable to remark the high sensitivity of the optical probe techniques, as power dissipation magnitudes in the order of 50 μW to 300 μW were expected from simulation for the spectral component of the power dissipated by the transistor MNC at the frequency (f_2-f_1), causing temperature increases in the mK range.

7. Conclusions

In this paper we have shown that temperature can be used as an alternative observable for some figures of merit of analog and RF blocks. The use of optical techniques described here allows us to increase the observability of buried blocks, being useful to debug complex RF ICs, to estimate the effects of process variations, the accuracy of design models or the presence of parametric faults. Experimental results obtained with a laser probe as thermometer have been shown. However, the technique is fully compatible with other temperature sensing strategies, such as embedded temperature sensors or IR lock-in thermography. Laser probing allows high sensitivity temperature measurements at any place of the IC layout without loading effect on the CUT. We have experimentally proved that we can observe the frequency response of a RF LNA in the range of 500 MHz to 1.10 GHz by performing low frequency (1 kHz and 5 kHz) temperature measurements.

Acknowledgment

The authors wish to thank Dr. J. Puigdollers and Dr. E. Alarcón for providing with necessary laboratory equipment. This work was supported in part by TEC2005-06784-C02-01MIC, TEC2005-02739MIC, the integrated action HF2004-0042 of Spanish MEC and FEDER founds. E. Aldrete thanks the support of DURSI-Generalitat de Catalunya (2007FIR00120). We thank the MOSIS Educational Program for IC prototype fabrication.

References

[1] K.B. Schaub, J. Kelly, "Production Testing of RF and System-on-a-Chip Devices for Wireless Communications", Artech House, Boston, 2004.

[2] J. Machado da Silva, "A Low Power Oscillation Based LNA BIST Scheme," *International Conference on Design and Test of Integrated Systems in Nanoscale Technology,* Sep. 2006, Gammarth, Tunisia, pp. 268 -272.

[3] J. Liobe, M. Margala, "Fault diagnosis of a GHz CMOS LNA using high-speed ADC-based BIST," in *Proceedings of the IEEE International Workshop on Current and Defect Based Testing*, April 2004, pp. 85-89.

[4] J. Dabrowski, "BiST model for IC RF-transceiver front-end," in *Proceedings of the 18th IEEE International Symposium on Defect and Fault Tolerance in VLSI Systems*, November 2003. pp. 672-679.

[5] J. -Y. Ryu, and B.C. Kim, "A new design for built-in self-test of 5GHz low noise amplifiers," in *Proceedings of the IEEE International SOC Conference*, September 2004, pp.324-327.

[6] S. Bhattacharya, and A. Chatterjee "Use of Embedded Sensors for Built-In-Test of RF Circuits," in *Prceedings of the International Test Conference,* 2004, pp. 801-809.

[7] A. Gopalan, T. Das, C. Washburn, P. R. Mukund, "An ultra-fast, on-chip BiST for RF low noise amplifiers," *18th International Conference on VLSI Design*, January 2005, pp. 485-490.

[8] J.M. Soden, R.E. Anderson, "IC Failure Analysis: Techniques and Tools for Quality and Reliability Improvement*," Proceedings of the IEEE.* Vol. 81, no. 5, pp. 703-715, May 1993

[9] D. L. Blackburn, "Temperature measurements of semiconductor devices – a review", *20th SEMITHERM Symposium,* 9-11 Mar 2004, pp. 70-80, 2004.

[10] J. Altet, W. Claeys, S. Dilhaire, A. Rubio, "Dynamic Surface Temperature Measurements in ICs ", *Proceedings of the IEEE*, Vol 94, No. 8, August 2006, pp. 1519-1533.

[11] D. Mateo, J. Altet, E. Aldrete-Vidrio, "Electrical characterization of analogue and RF integrated circuits by thermal measurements" *Microelectronics Jounal*, vol. 38, no. 2, Feb. 2007, pp. 151-156

[12] D. Mateo, J. Altet, E. Aldrete-Vidrio, "An approach to the electrical characterization of analog blocks through thermal measurements", *In Proceedings 11th THERMINIC Workshop,* Sep. 2005, pp. 59-64.

[13] T. H. Lee, The Design of CMOS Radio-Frequency Integrated Circuits, Chapter 11, Cambridge University Press, 1998.

[14] S. Dilhaire, S. Grauby, S. Jorez, L.D. Patiño Lopez, E. Schaub and W. Claeys, "Laser diode COFD analysis by thermoreflectance microscopy", *Microelectronics Reliability*, vol. 41, pp. 1597-1601, 2001.

[15] V. Quintard, G. Deboy, S. Dilhaire, D. Lewis, T. Phan, W. Claeys, "Laser beam thermography of circuits in the particular case of passivated semiconductors," *Microelectronic Engineering* 31 (Elesevier), pp. 291-298, 1996.

[16] W.Claeys, S. Dilhaire, S. Jorez, L. Patiño-López, " Laser probe for the thermal and thermomechanical characterisation of microelectronic devices," *Microelectronics Journal*, vol. 32, pp. 891–898, 2001.

[17] N. Nenadovic, S. Mijalkovic, L.K. Nanver, L.K.J. Vandamme, V. d'Alessandro, H. Schellevis, J.W. Slotboom, "Extraction and modeling of self-heating and mutual thermal coupling impedance of bipolar transistors," *IEEE J. Solid-State Circuits*, Vol. 39, issue 10, Oct 2004, pp. 1764–1772.

[18] R. Ramzan, L. Zou, and J. Dabrowski, "LNA Design for on-chip RF test," in *Preceedings of IEEE International Symposium on Circuit and Systems*, 2006, pp. 4236-4239.

[19] M. Cimino, H. Lapuyade, M. De Matos, T. Taris, Y. Deval, and L. B. Begueret, "A Sub 1V CMOS LNA dedicated to 802.11/g applications with self-test & high reliability capabilities," in Proceedings of IEEE Radio Frequency Integaretd Circuits Symposium, 2007, pp. 343-346.

[20] H. Yen-Chih. H. Hsieh-Hung, and L. Liang-Hung, "A Low-Noise Amplifier with Integrated Current and Power Sensors for RF BIST Applications," presente at 25th IEEE VLSI Test Symposium, 2007, pp. 401-408.